Experimental Cell Research 381 (2019) 280–287

Contents lists available at ScienceDirect

Experimental Cell Research

journal homepage: www.elsevier.com/locate/yexcr

The paracrine effects of fibroblasts on Doxorubicin-treated breast cancer cells

Carla Fourie*, Tanja Davis, Jurgen Kriel, Anna-Mart Engelbrecht

Department of Physiological Sciences, Stellenbosch University, Stellenbosch, 7600, South Africa

ARTICLE INFO

Keywords:
Apoptosis
Breast cancer
Doxorubicin
Fibroblasts
Senescence
Treatment resistance

ABSTRACT

Breast cancer is frequently diagnosed in women and poses a major health problem throughout the world. Currently, the unresponsiveness of cancer cells to chemotherapeutics is a major concern. During chemotherapeutic treatment with Doxorubicin, neighbouring cells in the tumor microenvironment are also damaged. Depending on the concentration of Doxorubicin, apoptotic or senescent fibroblasts in the tumor microenvironment can then secrete a variety of bioactive molecules which promote tumor growth, metastasis and drug resistance.

Mouse embryonic fibroblasts (MEFs) were treated with Doxorubicin to induce apoptosis and senescence respectively. Conditioned media was collected from the MEFs and was used to assess the paracrine effects between fibroblasts and E0771 murine breast cancer cells.

Senescent fibroblasts significantly increased cell viability in E0771 cells following Doxorubicin treatment by activating Akt and ERK. Autophagy contributed to cancer cell death and not to treatment resistance in breast cancer cells.

Our results highlight the complexity of the tumor microenvironment where chemotherapeutic agents such as Doxorubicin can induce significant changes fibroblasts which can affect tumor growth via the secretion of paracrine factors. Here we have demonstrated that those secreted paracrine factors enhance breast cancer growth and induce therapeutic resistance through the evasion of apoptotic cell death.

1. Introduction

Breast cancer is frequently diagnosed in women worldwide, where 2.1 million cases of breast cancer were diagnosed during 2018 [1]. Different gene mutations result in the onset of different breast cancer subtypes, which makes it difficult to determine the exact diagnosis as well as treatment options that will be most successful in eliminating the cancer [2]. The focus of breast cancer research has been on the transformed tumor itself, but recently the surrounding tumor microenvironment (TME) is being extensively investigated because of its contribution to chemotherapeutic resistance [3,4]. The TME is characterized by cellular and non-cellular components of the tumoral niche, which includes extracellular matrix (ECM) components, lymphatic vascular networks, fibroblasts, immune cells and adipose cells [5,6]. These cells are often recruited to the primary tumor site to establish the TME for tumor progression in soluble paracrine signals, which contribute to the rapid growth of cancer cells, advanced stage malignancies and metastasis, thereby enhancing the complexity of breast cancer treatment strategies.

Breast stroma is characterized by many cell types, including macrophages, adipocytes and fibroblasts [7]. Under normal physiological conditions, fibroblasts maintain physiological homeostasis by regulating ECM turnover and wound healing. The interaction between breast stroma and epithelial cells is therefore critical for proper breast development [8].

Doxorubicin (DXR), an anthracycline, is an effective anti-cancer chemotherapeutic commonly used to treat a wide spectrum of cancers including leukaemia, lung, breast, stomach and ovarian cancer and is currently one of the most potent anti-tumor antibiotics [9,10]. The proposed main mechanism of action for DXR is the ability to poison topoisomerase II within the nucleus of cancer cells [11]. However, the exposure to DXR can induce a senescent state in a variety of cells including cancerous and non-cancerous cells, depending on the dosage and treatment duration.

Abbreviations: CM, Conditioned media; DXR, Doxorubicin; ECM, Extracellular matrix; MEFs, mouse embryonic fibroblasts; PBS, Phosphate buffered saline; RB, Retinoblastoma; SA-β-ga, Senescence-associated-beta-galactosidase; TME, Tumor microenvironment

* Corresponding author. Merriman and Bosman Street Mike de Vries Building, Stellenbosch, 7600, South Africa.
E-mail addresses: carlafourieSU@gmail.com (C. Fourie), tadavis@sun.ac.za (T. Davis), 16635337@sun.ac.za (J. Kriel), ame@sun.ac.za (A.-M. Engelbrecht).

https://doi.org/10.1016/j.yexcr.2019.05.020
Received 17 April 2019; Received in revised form 14 May 2019; Accepted 16 May 2019
Available online 20 May 2019
0014-4827/

Senescence, which was first introduced by Hayflick and Moorhead, is defined as a permanent growth arrest that occurs in cells, which remain metabolically active, but display changes in morphology [12]. Accelerated or oncogene-induced senescence can be induced by external stressors like chemotherapeutic drugs, including DXR [13]. The anti-proliferative nature of the senescence response clearly highlights the plausible effect of a tumor suppressor mechanism because of its ability to inhibit malignant transformation and growth. However, extensive research has indicated that senescent cells develop altered secretory activities in the TME, which can promote tumorigenesis. In cell culture models, cancer cell growth is promoted by paracrine factors like cytokines (interleukin-1 and interleukin-6) secreted from senescent fibroblasts, by enhancing the proliferation and blocking programmed cell death in cancer cells [14,15]. The phenomenon where senescent cells remain metabolically active but undergo changes in protein secretion and expression, is referred to as the senescence-associated secretory phenotype (SASP) [16]. The SASP is constituted of many soluble and insoluble factors that affect neighbouring cells through the activation of cell surface receptors and signal transduction pathways. Once the SASP is induced in cells, the cells undergo stable cell cycle arrest as well as morphological changes associated with cellular senescence [17,18]. These changes include a flat and enlarged cellular morphology and the upregulation of senescence-associated β-galactosidase activity. A persistent DNA damage response (DDR) contributes to the onset of the senescent phenotype by upregulating p21 and p16 (cyclin-dependent kinase inhibitors) as well as the consequent activation of the retinoblastoma tumor suppressor protein to induce irreversible cell cycle arrest [19]. *In vitro* studies have confirmed that the proliferation of a cancer cell line is enhanced by conditioned media generated from senescent fibroblasts [20].

Autophagy, a type of programmed cell death that maintains the turnover of organelles and proteins, is also activated by the significant changes in cytokine expression [21]. The process of autophagy is involved in many biological processes, including cell death or survival, proliferation, senescence and the onset of carcinogenesis [22]. However, the role of autophagy in cancer remains controversial [23]. Proliferating tumor cells are highly disadvantaged once autophagy is inhibited because compensatory mechanisms must be implemented for cancer cell survival [24].

The ability of cancer cells to develop chemotherapeutic resistance is still a major concern. The effectiveness of current cancer therapies is limited once cancer cells are able to evade apoptotic cell death. Therefore, combination therapy or therapeutic options that target alternative pathways should be considered.

Since fibroblasts in the TME are influenced by DXR during breast cancer treatment, the aim of this study was to assess the effects of apoptosis and senescence conditioned media generated from fibroblasts on breast cancer cells to determine whether an apoptotic or senescent state in fibroblasts in the TME will influence the growth of breast cancer cells *in vitro*. In this study, we demonstrate the detrimental outcome that senescent fibroblasts can have on the success rate of chemotherapeutic treatment, specifically DXR.

2. Materials and methods

2.1. Cell lines and chemicals

Mouse embryonic fibroblasts (MEFs) kindly received from Prof Ben Loos (Stellenbosch University, Cape Town, South Africa) and mouse E0771 breast cancer cells provided by Prof Fengzhi Li (Roswell Park Cancer Institute, Buffalo, New York, USA) were cultured in Dulbecco's Modified Eagle's medium (DMEM) (Gibco), supplemented with 10% fetal bovine serum (FBS) (Capricorn Scientific) and 1% penicillin-streptomycin (Gibco). All cells were incubated in a 5% CO_2 incubator at 37 °C. DXR hydrochloride (Sigma) was prepared in a stock solution by dissolving it in pure DMEM. Aliquots were stored at −20 °C and further dilutions were made in culture medium. Bafilomycin (LKT Laboratories) was stored in aliquots at −20 °C and dilutions were made in culture medium.

2.2. Senescence associated β-galactosidase stain

MEFs were seeded and treated with 2 μM of DXR for 4 h. After the treatment period, the cells were incubated for 12 days in a 5% CO_2 incubator at 37 °C. Detection of SA-β-galactosidase activity was performed as previously described [25] on day 12 and the cells were incubated for 16 h. Images were obtained by a brightfield microscope at 40× magnification and six images per group were obtained. Cells were counted by using ImageJ software.

2.3. Conditioned media

MEFs were treated with 2 μM DXR for 4 h and incubated for 13 days. Conditioned media (CM) was collected and centrifuged at 5000 rpm for 10 min at 4 °C on day 7, 10 and 13 and was filtered with a 0.2 μm filter. For apoptosis, MEFs were treated with 1 μM DXR for 24 h where after the media was collected and centrifuged at 5000 rpm for 10 min at 4 °C. The CM was snap frozen in liquid nitrogen and stored at −80 °C.

2.4. MTT assay

E0771 cells were treated with DXR-induced apoptotic and senescence CM generated from MEFs for 24 h. At the end of the treatment duration, MTT solution, dissolved in 0.1 M PBS, was added and incubated for one hour in a 5% CO_2 incubator at 37 °C before solubilization. Absorbance was measured at 595 nm in a microplate reader.

2.5. Western blot

Total cell protein was extracted by incubating the cells in radioimmuno precipitation (RIPA) buffer. Protein quantification was performed by using a Bradford assay [26]. Samples (50 μg/lane) were subjected to 12% SDS-PAGE and transferred to a PVDF membrane (Biorad). The membrane was then probed with primary antibodies overnight, incubated in secondary antibody for 1 h at room temperature the following day and visualized by ECL (Biorad). The following primary antibodies were used: Caspase 3 (Abcam; #ab184787; 1:1000), Caspase 8 (Abcam; #ab25901; 1:1000), Caspase 9 (CST; #9508 1:500), PARP (Abcam; #ab191217; 1:500), MCM2 (Abcam; #ab108935; 1:10 000), p53 (Invitrogen; #13-4100; 1:500), p21 (Invitrogen; #AHZ0422; 1:500), p16 (Abcam; #ab189034; 1:1000), RB (Abcam; #ab181616; 1:1000), LC3II (CST; #3868; 1:1000), p62 (Abcam; #ab109012; 1:1000), Akt (CST; #9272; 1:1000) and ERK (Abcam; #ab184699; 1:1000). For protein quantification, the relative amount of each protein investigated was normalized to the total protein signal in each lane using Image Lab software™ (Biorad) as determined by the Stain-Free™ properties of the blot.

2.6. Immunofluorescence

E0771 breast cancer cells were grown on coverslips and treated with CM, DXR and Bafilomycin (400 nM, 4 h prior to the end of the treatment duration) for 24 h. After the treatment period, cells were washed with ice-cold PBS and fixed for 10 min in 4% paraformaldehyde, followed by permeabilization with 0.1% Triton-X (Sigma Aldrich) for 10 min. Afterwards, the cells were blocked in 1% BSA (Roche) for 60 min and incubated in primary antibodies, p62 (Abcam; #ab109012; 1:400) and LC3 II (CST; #3868; 1:200) overnight. The cells were then washed with PBS and incubated in secondary antibody (Donkey anti-Rabbit IgG (H + L) Secondary Antibody Alexa Fluor 568 [ThermoFisher Scientific, #A10042]) prepared in PBS for 60 min. Hoechst 33 342 (1:200, Sigma Aldrich) was used for nuclear staining. Cells were

visualized with the Olympus® Cell^R system on an Olympus® IX81 inverted fluorescence microscope (Olympus®, GMBH Japan) using the 60× oil immersion objective and the 360 nm and 492 nm excitation filters. For image processing, Z-stacks were 3D deconvoluted with Huygens Professional software (Version 18.10, Scientific Volume Imaging, http://svi.nl). 2D maximum intensity projections were produced from deconvoluted z-stacks and adaptive Otsu thresholding was applied to each image with a threshold smoothing scale of 0.5 and a threshold correction factor of 2.0 (CellProfiler 3.1.5.1). LC3 and p62 positive structures were then quantified through particle counts using Fiji (Image J) software2.

2.7. Statistical analyses

Statistical analyses were performed using GraphPad version 5.0 statistical software. The significance was calculated using student t-tests and one-way analysis of variance (ANOVA), followed by a Bonferroni post-hoc test. All results are expressed as mean ± standard error of the mean (SEM). A p-value less than 0.05 was considered statistically significant.

3. Results

3.1. DXR induced apoptosis activation in MEFs

MEF cell viability was significantly decreased when treated with DXR concentrations ranging between 1 to 10 μM (Fig. 1). To confirm the induction of apoptosis in DXR-treated MEFs, the expression of several apoptotic markers was measured by western blotting. The expression of Caspase 3 (Fig. 2A), Caspase 8 (Fig. 2B), Caspase 9 (Fig. 2C) and PARP (Fig. 2D) was assessed after the 24-h treatment period with 1 μM DXR. As shown in Fig. 2A and B, cleaved caspase 8 and caspase 3 was significantly increased after the treatment period. Interestingly, cleaved PARP was significantly decreased in the DXR treated group when compared to the control (Fig. 2D). However, no changes in the expression of Caspase 9 was observed (Fig. 2C). From this data, we concluded that DXR efficiently induces apoptotic cell death in MEFs by activating the extrinsic apoptosis pathway.

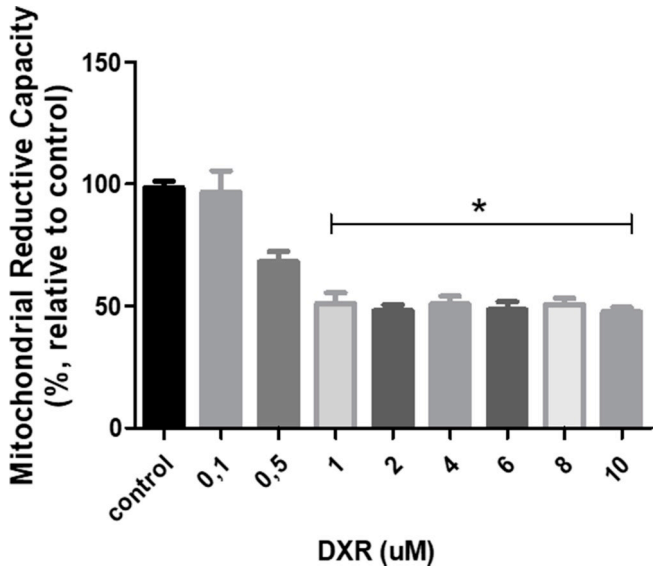

Fig. 1. Percentage viability of MEFs after a DXR treatment period determined by an MTT assay. MEFs were seeded and treated with different DXR concentrations over a period of 24 h. Results are presented as means ± SEM (n = 3). The (*) denotes a significant decrease in cell viability when compared to the control.

3.2. DXR induced senescence in MEFs

A SA-β-gal assay (Fig. 3) was used to determine the amount of senescence induced in a MEF population. MEFs were treated with 2 μM of DXR for 4 h, followed by a 12-day incubation period. After the treatment period, 56% of the MEF population was senescent. After the incubation period, Western blot analyses was used to confirm that the MEFs were senescent and non-proliferative. MCM2 (Fig. 4A) was significantly decreased on day 8 and day 12 when compared to the control. p16 (Fig. 4B) and total RB (Fig. 4C) was also significantly increased on day 12. Based on these results, we concluded that a senescent state had been successfully induced in a MEF population.

3.3. Effects of conditioned media on E0771 cells

Next, we investigated the sensitivity of E0771 mouse breast cancer cells to DXR in the presence of apoptotic and senescent CM by using an MTT assay. Cell viability was assessed after E0771 cells were treated with apoptotic and senescent CM in the presence of 1 μM DXR for 24 h (Fig. 5). Senescent CM with DXR (CM-S-DXR) showed significantly less cell death when compared to both the control and apoptotic CM (CM-C-DXR and CM-A-DXR). This data indicates that E0771 cells evade cell death and possibly enhance their proliferative capacity in the presence of senescence CM even after DXR had been administered, which can ultimately contribute to treatment resistance. To determine if E0771 cells evade cell death the expression of apoptotic markers was analysed by Western blot. Cleaved caspase 8 (Fig. 6A) as well as caspase 3 (Fig. 6B) was significantly decreased in CM-S-DXR. Total PARP (Fig. 6C) expression was also significantly decreased in senescence CM. This data leads us to believe that senescent fibroblasts secrete certain factors that allow E0771 cells to evade apoptosis and induce treatment resistance.

3.4. E0771 cells have enhanced proliferation capacity

The expression of MCM2 was used to investigate whether the E0771 cells are in a proliferative state after a 24-h treatment period with senescence CM and DXR (CM-S-DXR). MCM2 was significantly increased in senescence CM (CM-S) as well as senescence CM in the presence of DXR (CM-S-DXR) (Fig. 7A). Furthermore, p53, a tumor suppressor protein, was significantly increased in apoptosis CM in the presence of DXR (CM-A-DXR) (Fig. 7D). However, contradictory to the increased expression of MCM2, p16 and total RB was significantly increased in senescence CM in the presence of DXR (CM-S-DXR) (Fig. 7B and C). Based on these results, the increased expression of MCM2 indicates that E0771 cells remain proliferative by factors secreted from senescent fibroblasts.

3.5. Autophagy contributes to E0771 cell death

To investigate whether autophagy contributes to E0771 cells evading apoptotic cell death, an MTT assay was used. In the presence of Bafilomycin A1 (a late phase autophagy inhibitor), cell viability was significantly decreased in the control CM (CM-C-Baf), but was significantly increased in apoptosis (CM-A-Baf) and senescence CM (CM-S-Baf) when compared to the respective groups without Bafilomycin (Fig. 8). Based on these results, we concluded that autophagy has a cytotoxic role in E0771 cells during treatment with apoptotic and senescent CM because of its contribution to cell death.

3.6. DXR does not induce changes in autophagic flux

The expression of LC3 II and p62 was analysed by Western blot to investigate the role of autophagy in treatment resistance (Fig. 9). In the presence of Bafilomycin A1, the expression of LC3 II was significantly increased in control, apoptosis and senescence CM (Fig. 9A).

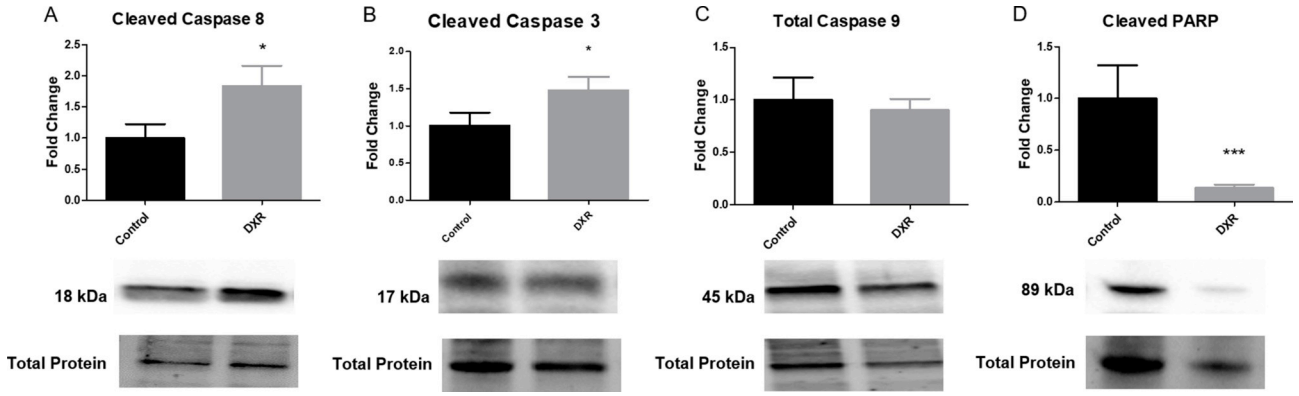

Fig. 2. Effect of DXR on apoptosis activation in MEFs. The expression of the indicated proteins was examined by western blotting in MEFs: (A), Cleaved Caspase 8, (B), Cleaved Caspase 3, (C) Caspase 9 and (D) Cleaved PARP after a 24-hr treatment period with 1 μM DXR. Total protein was used for normalization. The (*) denotes a significant difference when compared to the control.

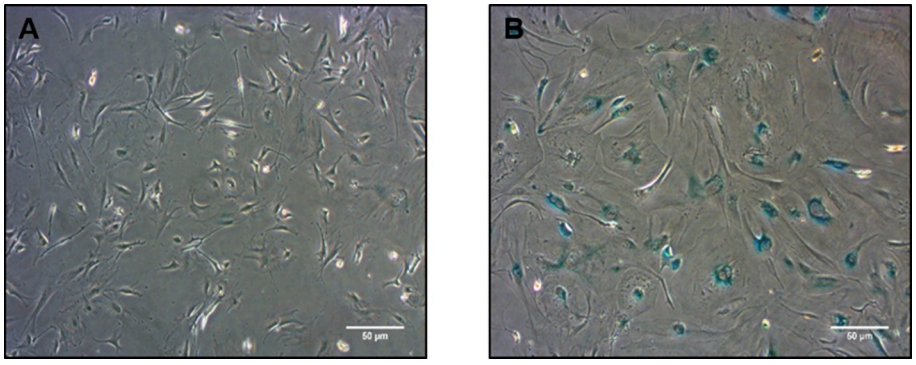

Fig. 3. Phenotypical changes in MEFs following treatment with DXR for senescence induction as determined by a SA-β-gal assay. MEFs were treated with DXR (2 μM) for 4 h followed by a 12-day incubation period under normal culture conditions. Fig. 2A represents an untreated control MEF group. MEFs were stained on day 12 for 16 h before acquiring the images with a bright field microscope (Fig. 2B). Three independent experiments were performed.

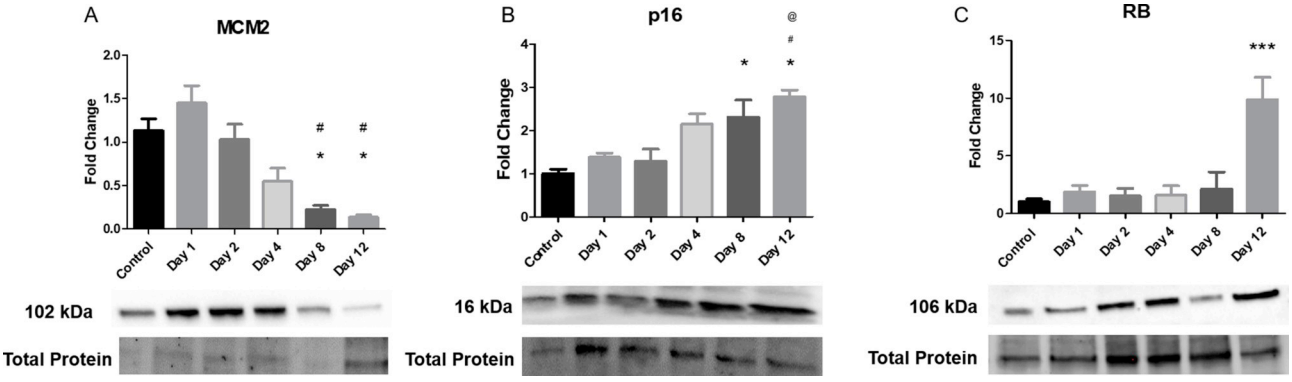

Fig. 4. Effect of DXR on senescence induction in MEFs. The expression of the indicated proteins was examined by western blotting in MEFs: (A), MCM2, (B), p16 and (C) total RB after a 4-hr treatment period with 2 μM DXR. Total protein was used for normalization. The (*) denotes a significant difference when compared to the control; (#) denotes a significant difference compared to day 1 and (@) denotes a significant difference compared to day 2.

Autophagic flux as defined by du Toit et al. [27] was used to measure autophagic degradation activity. However, no changes in the expression of LC3 II to indicate that autophagic flux was occurring, was observed. Furthermore, similarly to LC3 II, the observed expression of p62 (Fig. 9B) indicated that no changes in autophagic flux was occurring. Autophagosome counts were then performed by immunocytochemistry analysis (Fig. 10). However, no changes to indicate that autophagic flux had occurred was observed.

3.7. Senescent fibroblasts enhance proliferation of E0771 cells

To investigate possible mechanisms for E0771 proliferation following treatment with senescent CM, key signaling proteins were assessed by western blotting. The activation of Akt (Fig. 11A) was significantly increased in CM-A-DXR, CM-S and CM-S-DXR. Similarly, a significant increased activation of ERK (Fig. 11B) was observed in CM-A-DXR and CM-S-DXR. These results provide further evidence for cancer cell proliferation.

4. Discussion

In this study, we have shown that senescent fibroblasts contribute to the ability of mouse breast cancer cells to evade apoptotic cell death which contributed to chemotherapeutic resistance. DXR induces ROS production, which plays an important role in caspase activation to serve as primary mediators for the apoptotic pathway [28]. We and others have demonstrated that cleaved caspase 3 and caspase 8 was significantly increased in DXR treated MEFs following the treatment period [29,30]. These findings suggest that apoptosis had successfully been induced in the fibroblast population. The amount of senescence

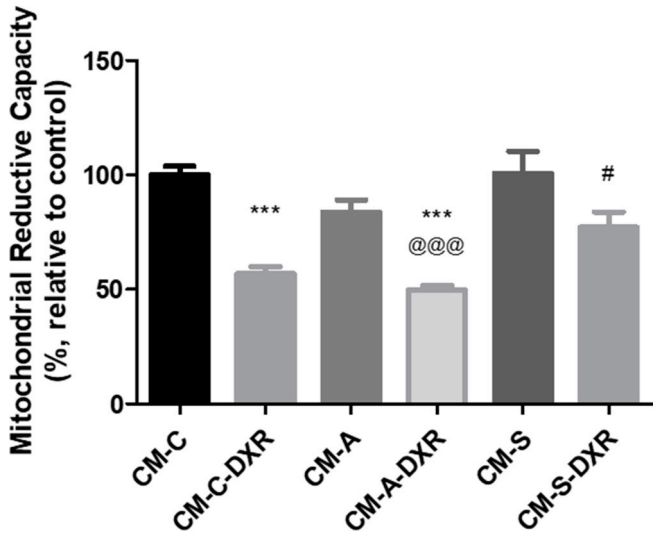

Fig. 5. The effects of conditioned media and DXR on E0771 cell death was measured by an MTT assay. E0771 cells were treated with CM with or without 1 μM DXR for 24 h. Error bars indicate mean ± SEM of three independent experiments. CM-C: conditioned media from fibroblasts untreated, CM-C-DXR: conditioned media from fibroblasts treated with DXR, CM-A: conditioned media from apoptosis-induced fibroblasts untreated, CM-A-DXR: conditioned media from apoptosis-induced fibroblasts treated with DXR, CM-S: conditioned media from senescence-induced fibroblasts untreated & CM-S-DXR: conditioned media from senescence-induced fibroblasts treated with DXR. The (*) denotes a significant decrease relative to the control; the (@) denotes a significant decrease relative to CM-A and (#) denotes a significant increase in CM-S-DXR relative to CM-C-DXR and CM-A-DXR.

(56%) in the MEF population was less than the recommended 80% suggested in literature, but still induced significant changes in E0771 cells [31]. The non-proliferative state of the MEFs was further supported by the decreased expression of MCM2 as well as the increased expression of two tumor suppressor proteins, p16 and total RB, both serving as markers of senescence.

Our results indicate that in the presence of DXR, conditioned media generated from senescent cells, induced evasion of apoptotic cell death in mouse breast cancer, as confirmed by the cell viability assay. This was supported by the decreased expression of several apoptotic markers including caspase 3, caspase 8 and PARP in the E0771 cells treated with DXR as well as the increased expression of MCM2, a DNA replication factor [32], which supports the enhanced proliferative ability of the cancer cells. Contradictory to the increased expression of MCM2 however, p16 and RB was significantly increased, which remains to be elucidated. The transition from the first growth phase (G1) to the synthesis phase (S-phase) is regulated by the p16-RB pathway. p16 binds to and inhibits cyclin-dependent kinase 4 (CDK4) activity, which blocks RB phosphorylation to prevent the G1/S-phase transition from occurring. Although a feedback loop exists between p16 and RB, it has been shown that the expression level of p16 does not change significantly during the cell cycle to correlate with RB expression, which is supported by the increase in p16 in RB-negative cells [33]. Therefore, further analysis needs to be implemented to determine other mechanisms of p16 regulation, which could potentially explain why the increase in the expression of these tumor suppression proteins were observed.

The physiological characteristics of the TME differ from those of normal tissue and is often described as hypoxic, nutrient deprived and inflammatory. These characteristics can induce autophagy through the activation of several pathways [34]. Autophagy is a normal physiological process that maintains cellular homeostasis by digesting damaged cellular components in lysosomes [35]. Basal levels of autophagy are found in all cell types, but can also be induced by external stressors like chemotherapeutic drugs [36,37]. As determined by an MTT assay, cell viability was increased in control CM in the presence of Bafilomycin A1, but was significantly decreased in apoptosis and senescence CM. These findings therefore suggest that autophagy had a cytoprotective role towards cancer cells in control CM and a cytotoxic role towards cancer cells in apoptosis and senescence CM. Autophagy was therefore contributing to cancer cell death and not treatment resistance. Although the expression of LC3 II, a marker for autophagosome formation, was increased in the presence of Bafilomycin no significant changes were observed to indicate that autophagic flux was occurring. Similarly, no significant changes in the expression of p62 were observed. Literature has suggested that changes in the expression of p62 is attributed to the ability of DXR to be sequestered into lysosomes, where it will be targeted to be degraded by autophagic machinery [38,39].

The expression of Akt and ERK activation were analysed to determine signaling pathways which are activated to induce cell proliferation in E0771 cancer cells treated with DXR. PI3K activation of Akt promotes the translocation of Akt from the cytosol to the plasma membrane and induces activation through phosphorylation at the Thr308 and Ser473 sites. Akt plays an important role in many intracellular signaling systems like cell growth, proliferation and apoptosis inhibition [40]. A significant increase in pAkt/total Akt was observed in CM-A, CM-A-DXR and CM-S with unchanged total levels of Akt, indicating that Akt activation had occurred. Furthermore, although total Akt expression was significantly increased in cells treated with control, apoptosis and senescence CM in the presence of DXR and Bafilomycin A1 decreased phosphorylation of Akt was observed in these

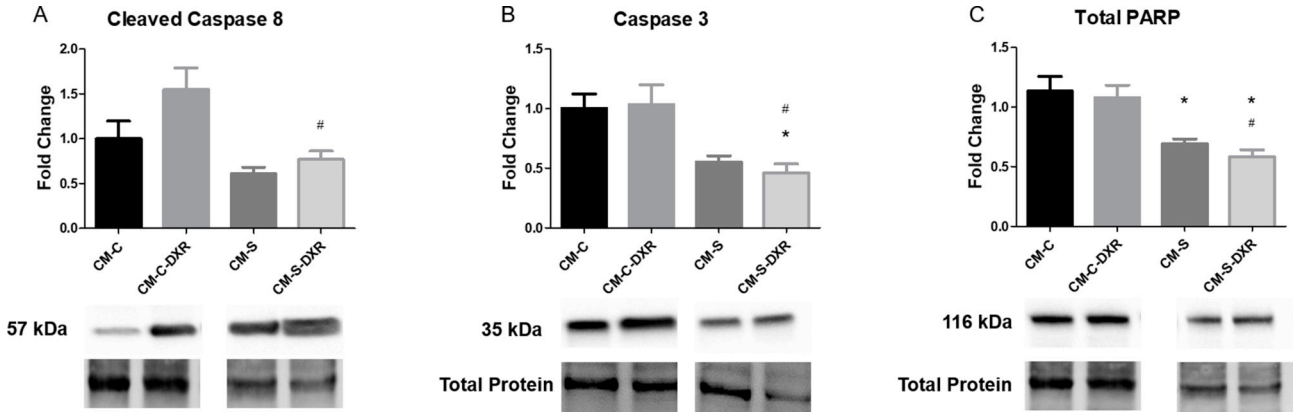

Fig. 6. Effects of CM and DXR on E0771 cell death. The expression of the indicated proteins was examined by western blotting in E0771 cells: (A), cleaved caspase 8, (B), caspase 3 and (C), PARP after a 24-hr treatment period with conditioned media and 1 μM DXR. Total protein was used for normalization. The (*) denotes a significant difference relative to the control and (#) relative to CM-C-DXR.

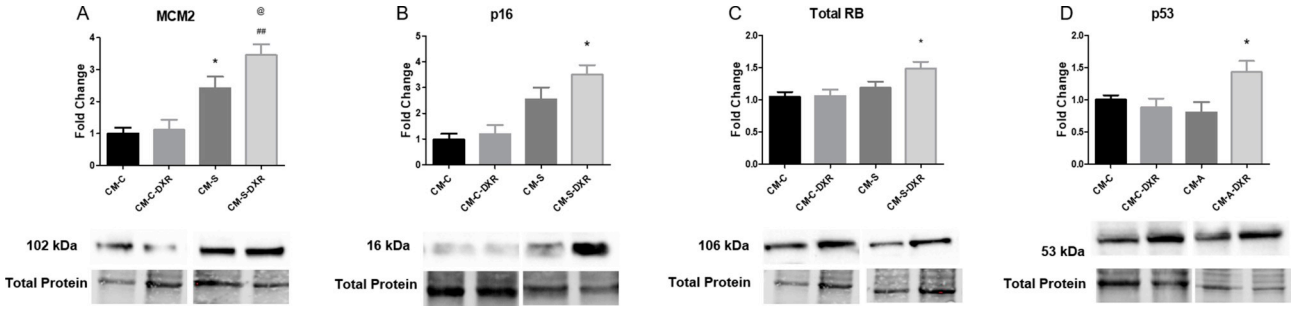

Fig. 7. Effects of CM and DXR on E0771 proliferation. The expression of the indicated proteins was examined by western blotting in E0771 cells: (A), MCM2, (B), p16, (C), total RB and (D) total RB after a 24-hr treatment period with conditioned media and 1 μM DXR. Total protein was used for normalization. The (*) denotes a significant difference relative to the control, (#) relative to CM-C-DXR and (@) relative to CM-S.

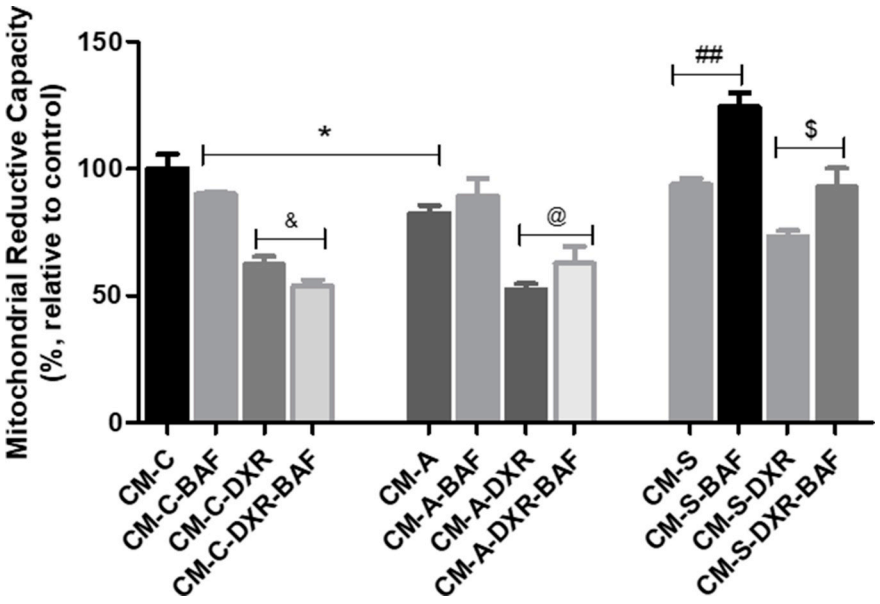

Fig. 8. The effects of conditioned media and DXR on E0771 cell death was measured by an MTT assay. E0771 cells were treated with CM with or without 1 μM DXR for 24 h and Bafilomycin A1 was added 4 h prior to the end of the treatment duration. Error bars indicate mean ± SEM of three independent experiments. The (*) denotes a significant decrease relative to the control, (&) denotes a significant decrease in CM-C-DXR-Baf relative to CM-CDXR; (@) denotes a significant increase in CM-A-DXR-Baf relative to CM-A-DXR; (#) denotes a significant increase in CM-S-Baf relative to CM-S and ($) denotes a significant increase in CM-S-DXR-Baf when compared to CM-C-DXR.

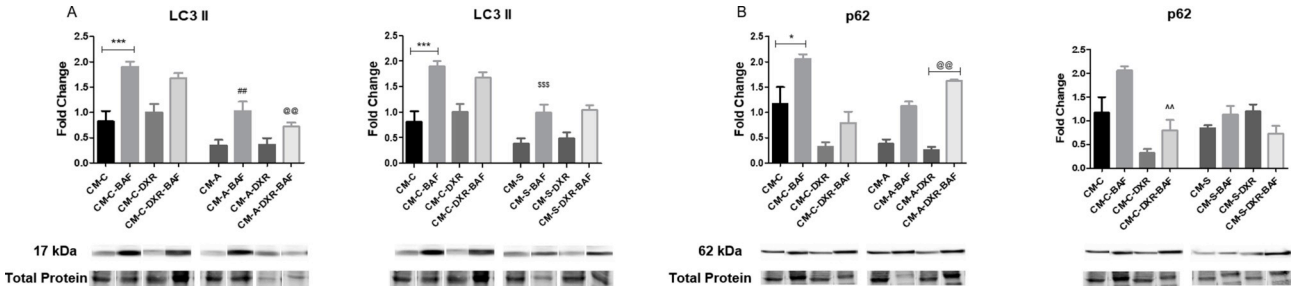

Fig. 9. Effects of CM, DXR and autophagy inhibition on E0771 cells. The expression of the indicated proteins was examined by western blotting in E0771 cells: (A) LC3 II and (B) p62 after a 24-hr treatment period with conditioned media, 1 μM DXR and 400 nM Bafilomycin A1. Total protein was used for normalization and bands were cropped to represent the group order as determined by the graphs. The (*) denotes a significant difference relative to the control, (#) relative to CM-A-Baf, (@) relative to CM-A-DXR, ($) relative to CM-S and (^) relative to CM-C-DXR.

groups, indicating lower Akt activation. ERK1/2 is a key signaling molecule that has been extensively investigated as a drug target for cancer therapy because of its ability to induce proliferation and malignant transformation of cancer cells [41]. The expression of pERK2/total ERK2 was significantly increased in cells treated with apoptosis and senescence CM in the presence of DXR, which could provide a rationale for the increase in cancer cell viability. Not many studies have focused on the relationship between autophagy and ERK, but it was indicated in one study that the cellular availability of autophagic structures determines the degree of ERK phosphorylation. The authors speculated that LC3-II-positive membranes and ATG5–ATG12-positive pre-autophagosomes could serve as cellular signaling platforms that would allow spatial coordination of the Raf-MEK-ERK cascade to facilitate ERK phosphorylation. The authors further indicated that an increase in cell death in autophagy deficient cells may have occurred from decreased ERK activity [42]. This phenomenon was also observed during our study where cell death was increased in control CM groups supported by the decreased expression of ERK in control CM treated with Bafilomycin A1.

In summary, our results indicate that once senescence is induced in fibroblasts, tumor resistance is enhanced and the breast cancer cells have the ability to evade apoptosis by upregulating Akt and ERK activation.

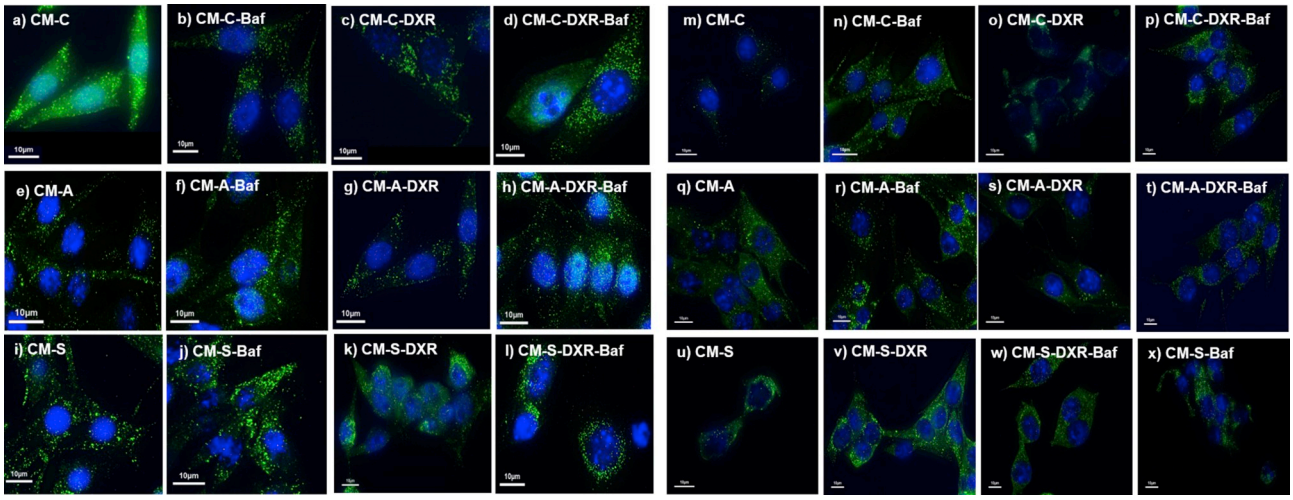

Fig. 10. Representative images of LC3 and p62 puncta in E0771 cells following CM and DXR treatment and autophagy inhibition. E0771 cells were seeded and treated with control CM (as previously described) and DXR for 24 h and Bafilomycin A1 was added 4 h prior to the staining protocol (a–d), (e–h) apoptosis CM and (i–l) senescence CM for LC3 II. The same protocol was followed for p62; (m–p), control CM, (q–t) apoptosis CM and (u–x) senescence CM.

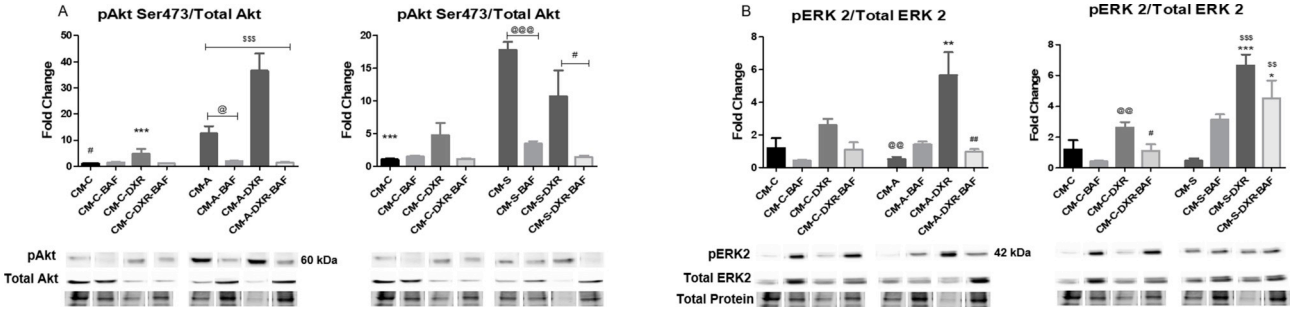

Fig. 11. Effects of CM, DXR and autophagy inhibition on E0771 proliferation. The expression of the indicated proteins was examined by western blotting in E0771 cells: (A) ERK2 and (B) Akt after a 24-hr treatment period with conditioned media, 1 μM DXR and 400 nM Bafilomycin A1. Total protein was used for normalization and bands were cropped to represent the group order as determined by the graphs. (A) For control and apoptosis CM the (*) denotes a significant decrease in CM-C-DXR when compared to CM-A-DXR, (#) denotes a significant decrease in CM-C when compared to CM-A, (@) denotes a significant decrease in CM-A-Baf relative to CM-A and ($) denotes a significant increase in CM-A-DXR. For control and senescence CM (*) denotes a significant decrease in CM-C when compared to CM-S, (@) denotes a significant increase in CM-S relative to CM-S-Baf and (#) denotes a significant increase in CM-S-DXR relative to CM-S-DXR-Baf. (B) For control and apoptosis CM (*) denotes a significant decrease in CM-C-DXR-Baf and all apoptosis CM, (#) denotes a decrease in CM-C-DXR-Baf when compared to CM-C-DXR and (@) denotes a decrease in CM-A-DXR when compared to CMC-DXR. For control and senescence CM (*) denotes a significant decrease in CM-C-DXR-Baf and in CM-S, CM-S-Baf and CM-C-DXR relative to the control, (#) denotes a decrease in CM-C-DXR-Baf when compared to CM-C-DXR and (@) denotes an increase in CM-S-DXR-Baf when compared to CM-C-DXR-Baf.

5. Conclusion

Senescent cells actively communicate with neighbouring cells and the TME, through the secretion of molecules that constitute the senescence associated secretory phenotype like cytokines, chemokines, and growth factors which can promote the proliferation of cancer cells. We have therefore clearly demonstrated that fibroblasts are influenced by DXR treatment to secrete factors which make cancer cells less susceptible to apoptotic cell death induced by chemotherapy.

Declarations of interest

None.

Acknowledgements

The authors acknowledge funding support from the Cancer Association of South Africa (CANSA), the National Research Foundation (NRF) and the Medical Research Council of South Africa (SAMRC).

References

[1] F. Bray, J. Ferla, I. Soerjomataram, R.L. Siegel, Global cancer statistics 2018: GLOBOCAN estimates of incidence and mortality worldwide for 36 cancers in 185 countries, A Cancer J. Clin. 107 (11) (2013) 843–847.
[2] A. Sims, Origins of breast cancer subtypes, Nature 4 (9) (2007) 516–525.
[3] M. Allinen, R. Beroukhim, L. Cai, C. Brennan, J. Lahti-domenici, H. Huang, D. Porter, M. Hu, Molecular characterization of the tumor microenvironment in breast cancer, Cancer Cell 6 (2004) 17–32.
[4] R. Eftekhari, R. Esmaeili, R. Mirzaei, K. Bidad, S. de Lima, M. Ajami, H. Shirzad, J. Hadjati, K. Majidzadeh-A, Study of the tumor microenvironment during breast cancer progression, Cancer Cell Int. 22 (17) (2007) 123.
[5] F. Chen, X. Zhuang, L. Lin, New horizons in tumor microenvironment biology: challenges and opportunities, BMC Med. 13 (45) (2015) 33.
[6] D. Hanahan, L.M. Coussens, Accessories to the crime: functions of cells recruited to the tumor microenvironment, Cancer Cell 21 (2012) 309–322.
[7] M.H. Barcellos-Hoff, S.A. Ravani, Irradiated mammary gland stroma promotes the expression of tumorigenic potential by unirradiated epithelial cells, Cancer Res. 60 (2000) 1254–1260.
[8] R. Kalluri, M. Zeisberg, Fibroblasts in cancer, Nat. Rev. Canc. 6 (5) (2006) 392–401.
[9] A.N. Gordon, Recurrent epithelial ovarian carcinoma: a randomized phase III study of pegylated liposomal doxorubicin versus topotecan, J. Clin. Oncol. 19 (14) (2001) 3312–3322.
[10] J.D. Bjorge, A.S. Pang, M. Funnell, K.Y. Chen, R. Diaz, A.M. Magliocco, D.J. Fujita, Simultaneous siRNA targeting of Src and downstream signaling molecules inhibit tumor formation and metastasis of a human model breast cancer cell line, PLoS One 26 (4) (2011) 6.

[11] D.A. Gewirtz, A critical evaluation of the mechanisms of action proposed for the antitumor effects of the anthracycline antibiotics adriamycin and daunorubicin, Biochem. Pharmacol. 57 (1999) 727–741.
[12] L. Hayflick, P.S. Moorhead, The serial cultivation of human diploid cell strains, Exp. Cell Res. 25 (3) (1961) 585–621.
[13] D.A. Gewirtz, S. Holt, L.W. Elmore, Accelerated senescence, Biochem. Pharmacol. 76 (2009) 947–957.
[14] D. Conze, L. Weiss, P. Regen, A. Bhushan, D. Weaver, P. Johnson, M. Rinco´n, Autocrine production of interleukin 6 causes multidrug resistance in breast cancer cells, Cancer Res. 61 (2001) 8851–8858.
[15] B. Chang, M.E. Swift, M. Shen, J. Fang, E.V. Broude, I.B. Roninson, Molecular determinants of terminal growth arrest induced in tumor cells by a chemotherapeutic agent, PLoS One 99 (1) (2002).
[16] J.P. Coppé, The senescence-associated secretory phenotype: the dark side of tumor suppression, Annu. Rev. Pathol. (5) (2010) 99.
[17] M. Serrano, A.W. Lin, M.E. McCurrach, D. Beach, S.W. Lowe, Oncogenic ras provokes premature cell senescence associated with accumulation of p53 and p16INK4a, Cell 88 (1997) 593–602.
[18] Y. Imai, i A. Takahash, A. Hanyu, Crosstalk between the Rb pathway and AKT signaling forms a quiescence-senescence switch, Cell Rep. 7 (2014) 194–207.
[19] N. Ohtani, K. Yamakoshi, A. Takahashi, E. Hara, The p16INK4a-RB pathway: molecular link between cellular senescence and tumor suppression, J. Medicat. Invest. 51 (2004) 146–153.
[20] J.P. Coppé, C.K. Patil, F. Rodier, Y. Sun, D.P. Muñoz, J. Goldstein, P.S. Nelson, P.Y. Desprez, Senescence-associated secretory phenotypes reveal cell non-autonomous functions of oncogenic RAS and the p53 tumor suppressor, PLoS Biol. 6 (12) (2008) 301.
[21] Z. Yang, D.J. Klionsky, Mammalian autophagy: core molecular machinery and signaling regulation, Curr. Opin. Cell Biol. 22 (2) (2010) 124–131.
[22] B. Levine, D.J. Klionsky, Development by self-digestion: molecular mechanisms and biological functions of autophagy, Dev. Cell 6 (2004) 463–477.
[23] M.C. Maiuri, E. Zalckvar, A. Kimchi, G. Kroemer, Self-eating and self-killing: crosstalk between autophagy and apoptosis, Nat. Rev. Mol. Cell Biol. 8 (2007) 741–752.
[24] L. Mah, K. Ryan, Autophagy and cancer, Cold Spring Harb. Perspect. Biol. 4 (2012) 8821.
[25] F. Debacq-Chainiaux, J.D. Erusalimsky, J. Campisi, O. Toussaint, Protocols to detect Senescence-associated-beta-galactosidase activity, a biomarker of senescent cells in culture and *in vivo*, Nature 4 (12) (2009) 1798–1806.
[26] M.M. Bradford, A rapid and sensitive method for the quantitation of microgram quantities of protein utilizing the principle of protein-dye binding, Anal. Biochem. 72 (1976) 248–254.
[27] A. Du Toit, J.S. Hofmeyer, T.J. Gniadek, B. Loos, Measuring autophagosome flux, Autophagy 14 (6) (2018) 1060–1071.
[28] M.C. Wei, T. Lindsten, V.K. Mootha, S. Weiler, A. Gross, M. Ashiya, C.B. Thompson, S.J. Korsmeyer, tBID, a membrane-targeted death ligand, oligomerizes BAK to release cytochrome c, Genes 14 (2000) 2060–2071.
[29] G. Nestal de Moraes, F. Vasconcelos, D. Delbuea, F. Mognol, C. Sternberg, R.C. Maiaa, Doxorubicin induces cell death in breast cancer cells regardless of Survivin and XIAP expression levels, Eur. J. Cell Biol. 92 (8) (2013) 247–256.
[30] S. Sharifi, J. Barar, i MJ. Hejaz, M. Samadi, Doxorubicin changes bax/Bcl-xL ratio, caspase-8 and 9 in breast cancer cells, Adv. Pharmaceut. Bull. 5 (3) (2015) 351–359.
[31] M. Demaria, M. O'Leary, J. Chang, L. Shao, S. Liu, F. Alimirah, K. Koenig, C. Le, N. Mitin, A.M. Deal, S. Alston, E.C. Academia, S. Kilmarx, A. Valdovinos, B. Wang, A. de Bruin, B.K. Kennedy, S. Melov, D. Zhou, N.E. Sharpless, H. Muss, J. Campisi, Cellular senescence promotes adverse effects of chemotherapy and cancer relapse, Cancer Discov. 7 (2) (2017) 165–176.
[32] I.T. Todorov, J. Lavigne, F. Sakr, R. Kaneva, S. Foisy, V. Bibor-Hardy, Nuclear matrix protein mitotin messenger RNA is expressed at constant levels during the cell cycle, Biochem. Biophys. Res. Commun. 177 (1) (1991) 395–400.
[33] H. Rayess, M.B. Wang, E.S. Srivatsan, Cellular senescence and tumor suppressor gene p16, Int. J. Cancer 130 (8) (2012) 1715–1725.
[34] R. Amaravadi, J. Lippincott-Schwartz, A. Yin, W. Weiss, N. Takebe, W. Timmer, R. DiPaola, M. Lotze, E. White, Principles and current strategies for targeting autophagy for cancer treatment, Clin. Cancer Res. 17 (4) (2011) 654–666.
[35] S. Rodriguez-Enriquez, L. He, J.J. Lemasters, Role of mitochondrial permeability transition pores in mitochondrial autophagy, Int. J. Biochem. Cell Biol. 36 (2004) 2463–2472.
[36] Y. Kondo, S. Kondo, Autophagy and cancer therapy, Autophagy 2 (2006) 85–90.
[37] M.C. Maiuri, E. Zalckvar, A. Kimchi, G. Kroemer, Self-eating and self-killing: crosstalk between autophagy and apoptosis, Nat. Rev. Mol. Cell Biol. 8 (2007) 741–752.
[38] A.A. Hindenburg, J.E. Gervasoni, S. Krishna, V.J. Stewart, M. Rosado, J. Lutzky, Intracellular Distribution and pharmokinetics of daunorubicin in anthracycline-sensitive and resistant HL60 cells, Cancer Res. 49 (1989) 4607–4614.
[39] H.M. Coley, W.B. Amos, P.R. Twentyman, P. Workman, Examination by laser scanning confocal fluorescence imaging microscopy of the subcellular localisation of anthracyclines in parent and multidrug resistant cell lines, Br. J. Canc. 67 (1993) 1316–1323.
[40] J. Downward, PI 3-kinase, Akt and cell survival, Semin. Cell Dev. Biol. 15 (2) (2004) 177–182.
[41] J.S. Sebolt-Leopold, Development of anticancer drugs targeting the MAP kinase pathway, Oncogene 19 (2000) 6594–6599.
[42] N. Martinez-Lopez, P. Mishall, R. Singh, Autophagy proteins regulate ERK phosphorylation, Nat. Commun. 4 (2013) 2799.